

## LONG TERM EVOLUTION OF PLANET-INDUCED VORTICES IN PROTOPLANETARY DISKS

WEN FU<sup>1,2</sup>, HUI LI<sup>2</sup>, STEPHEN LUBOW<sup>3</sup>, SHENGTAI LI<sup>2</sup>

<sup>1</sup>Department of Physics and Astronomy, Rice University, Houston, TX 77005, USA; wf5@rice.edu

<sup>2</sup>Los Alamos National Laboratory, Los Alamos, NM 87545, USA

<sup>3</sup>Space Telescope Science Institute, Baltimore, MD 21218, USA

*Draft version May 30, 2014*

### ABSTRACT

Recent observations of large-scale asymmetric features in protoplanetary disks suggest that large-scale vortices exist in such disks. Massive planets are known to be able to produce deep gaps in protoplanetary disks. The gap edges could become hydrodynamically unstable to the Rossby wave/vortex instability and form large-scale vortices. In this study we examine the long term evolution of these vortices by carrying out high-resolution two dimensional hydrodynamic simulations that last more than  $10^4$  orbits (measured at the planet's orbit). We find that the disk viscosity has a strong influence on both the emergence and lifetime of vortices. In the outer disk region where asymmetric features are observed, our simulation results suggest that the disk viscous  $\alpha$  needs to be low  $\sim 10^{-5}$  -  $10^{-4}$  to sustain vortices to thousands and up to  $10^4$  orbits in certain cases. The chance of finding a vortex feature in a disk then decreases with smaller planet orbital radius. For  $\alpha \sim 10^{-3}$  or larger, even planets with masses of 5 Jupiter-masses will have difficulty either producing or sustaining vortices. We have also studied the effects of different disk temperatures and planet masses. We discuss the implications of our findings on current and future protoplanetary disk observations.

*Subject headings:* accretion, accretion disks — hydrodynamics — instabilities — protoplanetary disks

### 1. INTRODUCTION

The new Atacama Large Millimeter/submillimeter Array (ALMA), although still at an early configuration, provides unprecedented resolution and sensitivity in the (sub)mm wavelength range. Recent high-fidelity ALMA images have revealed high contrast dust asymmetries in the outer parts of transitional disks around stars LkH $\alpha$  (Isella et al. 2013), Oph IRS 48 (van der Marel et al. 2013), HD 142527 (Casassus et al. 2013; Fukagawa et al. 2013), SAO 206462 and SR 21 (Pérez et al. 2014). These findings strongly suggest that the disk dust (and presumably gas) distribution is non-axisymmetric and the mechanisms for the generation and sustainment of these asymmetries need explanation.

Two scenarios have been suggested that could lead to strong asymmetries in protoplanetary disks, both of which use the excitation of Rossby wave instability (RWI Lovelace et al. 1999; Li et al. 2000). The RWI is a global non-axisymmetric instability which can be excited when there is a strong gradient and an inflexion point in the disk's radial potential vorticity profile. Many of the previous studies of RWI, in terms of both its linear stability properties and nonlinear evolution, used an assumed and idealized structure (such as a bump or an edge) in the disk radial density profile (Lovelace et al. 1999; Li et al. 2000; Meheut et al. 2010, 2012a,b,c, 2013; Richard et al. 2013). These structures, under appropriate conditions (as detailed in the linear theory calculations in Li et al. 2000), will form non-axisymmetric unstable modes. At the nonlinear stage, these non-axisymmetric modes develop into vortices and they further merge to form one large vortex (e.g. Li et al. 2001).

To explain the observed features in the transition disks, one scenario envisions that there exists sharp viscosity transitions in the radial direction of disks that may arise

near the edges of dead zones. Sharp viscosity change, thus sharp density change at outer edge of a dead zone can excite RWI (Regály et al. 2013; Lyra & Mac Low 2012). While the evolution of RWI will try to smooth out the density variation, the continuous accretion from material at large radii in the disk provides a driving effect on the RWI.

The other scenario is to explore the consequences of massive planets inside the disk (Lin & Papaloizou 1986a,b), especially in connection with the inner disk holes/cavities discovered in dozens of circumstellar disks (Forrest et al. 2004; Andrews et al. 2011; Espaillat et al. 2010; Kraus et al. 2013; Rosenfeld et al. 2013; Dodson-Robinson & Salyk 2011; Zhu et al. 2011; Kraus & Ireland 2012; Dobinson et al. 2013; Ruge et al. 2013). When a planet becomes massive enough, it carves out a deep gap around its orbit. Due to its significant density variations and the corresponding angular velocity adjustments, the gap edge can typically excite the RWI (e.g. Li et al. 2005), leading to the formation of vortices. Further nonlinear development of the RWI can lead to the formation of a “banana-shaped” asymmetric density enhancement (e.g. Li et al. 2005) or one large vortex (e.g. Lin & Papaloizou 2011; Lin 2012, 2014). One important condition for exciting RWI by a planet is that the disk viscosity needs to be sufficiently low, as it has been empirically studied by various groups (e.g. de Val-Borro et al. 2007; Li et al. 2009b; Yu et al. 2010; Lin & Papaloizou 2011). This scenario has been proposed to explain the ALMA observation of Oph IRS 48 (van der Marel et al. 2013), as well as the disk gap/hole (Ataiee et al. 2013).

These vortices are potentially very important because they can efficiently trap dust particles (e.g. Barge & Sommeria 1995; Johansen et al. 2004;

Inaba & Barge 2006; Rice et al. 2006; Meheut et al. 2012b; Pinilla et al. 2012; Zhu et al. 2012, 2014; Birnstiel et al. 2013; Lyra & Lin 2013), which in turn can produce asymmetric features in disk dust emission and help promote potential planet formation. Even though many previous studies have shown the generation of strong vortices in the disk, their long-term evolution, especially their survival time under different disk conditions, was left unaddressed. Though the exact lifetime of these vortices and/or asymmetric features is difficult to pin down observationally, the general expectation is that they need to survive up to  $\sim$  disk lifetime at tens of AU distances.

In this *Letter*, we present high-resolution, long-term two-dimensional simulations of disk-planet interactions that span  $> 10^4$  orbits at the location of vortex and we have explored the effects of several key disk/planet parameters on the vortex lifetime, including planet mass, disk viscosity, and disk temperature. In Section 2, we present the detailed set-up of our numerical simulations. We summarize our main results in Section 3, and discuss the implication of our results in Section 4.

## 2. NUMERICAL SETUP

In our study, the protoplanetary disks are assumed to be geometrically thin so that the hydrodynamical equations can be reduced to two-dimensional Navier-Stokes equations by considering vertically integrated quantities. We adopt an isothermal equation of state  $P = c_s^2 \Sigma$  where  $P$  is the vertically integrated pressure,  $\Sigma$  is the surface density and  $c_s$  is sound speed. Simulations are carried out using our code LA-COMPASS (Los Alamos Computational Astrophysics Suite).

The planet is taken to reside on a fixed circular orbit at radius  $r_p$  with Keplerian orbital frequency  $\Omega_p$ . We adopt dimensionless units in which the unit of length is  $r_p$  and the unit of time is  $1/\Omega_p$ . In dimensionless units, the disk is modeled between  $0.2 \leq r \leq 6.48$  with the planet at  $r = 1$ . We consider two mass ratios of the planet to the central star  $\mu = M_p/M_\star = 0.001$  and  $0.005$ , corresponding to a  $1M_J$  planet and a  $5M_J$  planet given a one solar mass central star. Planet mass is ramped up to its final value in the first 10 orbits. A smoothing length  $r_s = 0.6r_H$  is applied to the gravitational potential of the planet. We choose a power-law profile for both initial disk surface density and disk temperature of the form  $\Sigma \propto r^{-1}$ ,  $c_s \propto r^{-0.5}$ . The disk aspect ratio given by  $h/r = c_s/(\Omega r)$  is nearly independent of  $r$  (hereafter we will use  $h$  to stand for the dimensionless disk temperature). The initial disk mass is about  $1M_J$ . The dimensionless kinematic viscosity  $\nu$  (normalized by  $r_p^2 \Omega_p$ ) is taken to be spatially constant and ranges from  $\nu = 10^{-8}$  to  $\nu = 10^{-5}$ . The Shakura-Sunyaev viscosity is related to  $\nu$  by  $\alpha = \nu/(\Omega h^2)$ . All the simulations have a resolution of  $(n_r \times n_\phi) = 3072 \times 3072$ . The smallest Hill radius  $r_H = 0.07$  is thus resolved by 35 cells. We employ fixed value condition at boundaries. The initial disk surface density is completely smooth without an initial gap. Our simulations typically last for  $> 10^4$  orbits (at  $r = 1$ ).

## 3. RESULTS

Figure 1 shows the disk surface density evolution for two different planet masses. For a  $1M_J$  planet, a gap

in the disk can be developed quickly and the edges of the gap become unstable, giving rise to vortices that quickly merge into a single vortex. This type of behavior is quite general for all massive planet cases we have studied. This vortex can last for slightly more than  $10^3$  orbits (Fig. 1(c)), then it finally disappears (when azimuthal density variation across the vortex falls below  $\sim 10\%$ ).

For a  $5M_J$  planet (Fig. 1(d-f)), a single vortex remains robust at 5000 orbits and persists even after  $10^4$  orbits in Fig. 1(f). We see that after increasing the planet mass by a factor of 5, the vortex lifetime becomes almost 10 times longer for the same disk conditions. We expect the vortex survival time to increase with planet mass because a more massive planet is able to clear a deeper gap. The planet creates and maintains a sharper density jump at the gap edge that drives a stronger RWI. The vortex induced by the more massive planet covers a larger azimuthal range (see Fig. 1(b) and Fig. 1(e)).

Runs presented in Fig. 2 all have the same planet mass  $M_p = 5M_J$ , but different disk temperatures,  $c_s/\Omega|_{r=1} = h$ . Both cases have vortex lifetime only on the order of a few thousands of orbits. Together with Fig. 1(d-f),  $h = 0.06$  seems to be the optimal disk temperature for the purpose of disk vortex survival time. In that case, the vortex lifetime is  $\sim 13000$  orbits. We see that disk temperature has a very interesting nonmonotonic effect on the disk vortex lifetime. Either a higher or lower disk temperature results in more rapid vortex damping.

A similar effect can also be seen in Fig. 3 where we show runs with three additional disk viscosities ( $\nu = 10^{-5}$ ,  $10^{-6}$ ,  $10^{-8}$ ). Note that our code has numerical viscosity on the order of  $10^{-9}$  or less. For  $\nu = 1 \times 10^{-5}$  (first row), the disk is barely able to form a discernible nonaxisymmetric feature even though there seems to be a clean gap. Any vortex disturbance gets damped out in a very short time (a few hundreds of orbits). For  $\nu = 1 \times 10^{-6}$  (second row), the vortex evolution is very similar to that for  $\nu = 1 \times 10^{-7}$  (Fig. 1(d-f)), except that vortex lifetime is almost 10 times shorter. One would expect an even longer vortex lifetime for an even smaller viscosity because damping should decrease with smaller viscosity. Surprisingly, in the case of  $\nu = 1 \times 10^{-8}$  (third row), vortex lasts for significantly shorter time than in the case of  $\nu = 1 \times 10^{-7}$ . Therefore disk viscosity affects vortex lifetime also in a nonmonotonic way. A viscosity value  $\nu = 1 \times 10^{-7}$  seems to be optimal for vortex survival with  $M_p = 5M_J$  and  $h = 0.06$ . Vortex suppression at large disk viscosity has been found before (de Val-Borro et al. 2007; Li et al. 2009b; Lin & Papaloizou 2011; Isella et al. 2013; Ataiee et al. 2013). But previous studies have only considered  $\nu > 1 \times 10^{-7}$  and concluded the effect is monotonic. If viscosity is above some threshold ( $\sim 10^{-5}$  in our runs), vortex formation can also be completely suppressed. The dependence of vortex lifetime on viscosity and temperature is summarized in Fig. 4, which includes more cases than we presented in Figs. 1 and 2. We will give a tentative explanation for this behavior in Section 4.

We now consider the evolution of vortex in more detail. The upper part of Fig. 5 shows the evolution of  $\zeta(r, \phi)$  and  $\Sigma(r, \phi)$ , where  $\zeta = (\nabla \times \mathbf{v})_z/\Sigma$  is the po-

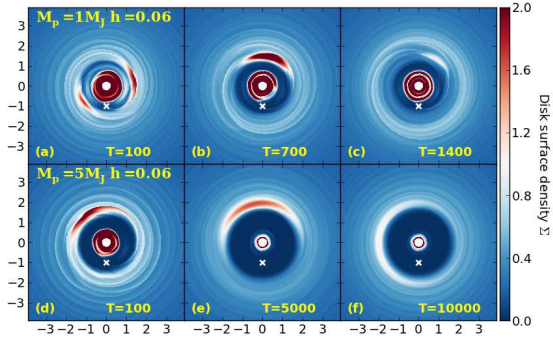


FIG. 1.— Evolution of disk surface density showing how the vortex develops and evolves for two different planet masses,  $M_p = 1M_J, 5M_J$ . Both runs employ disk viscosity  $\nu = 1 \times 10^{-7} r_p^2 \Omega_p$ . The location of the planet is marked by a white cross in every panel at dimensionless radius  $r = 1$ . Each row represents one simulation run with frames taken at different time points in units of planet orbital period. (Color online)

tential vorticity (PV). The vortex appears as a localized region of low PV (Fig. 5(a-c)) because the surface density is higher in those regions. To ease comparison, we have shifted the plots azimuthally so that the vortex is at the center in each Panel (a-c and d-f). Due to the large velocity perturbation and very low surface density, the PV within the gap region ( $(r - r_p)/h < 10$ ) is much higher than in other regions of the disk. We set an upper cutoff on our color scale in order to make the vortex more clearly visible. The lower part of Figure 5 shows the azimuthally averaged PV, defined as  $\langle \zeta \rangle = \langle (\nabla \times \mathbf{v})_z / \Sigma \rangle$ , and disk surface density  $\langle \Sigma \rangle$  profiles at different times. As the surface density profile associated with the gap widens due to the continuous driving by the planet (see the shift of in  $\langle \Sigma \rangle$  curves as a function of time), the minimum of PV profiles  $\langle \zeta \rangle$  also shifts to larger  $r$ , moving from  $(r - r_p)/h \sim 10$  at  $T = 100$  to  $(r - r_p)/h \sim 17$  at  $T = 5000 - 10000$ . Correspondingly, the radial location of the vortex also moved the same amount. This is quite consistent with the prediction of RWI theory where the disk vortex is formed where potential vorticity has a local minimum. In addition, from  $T = 100$  to  $T = 10000$ , the vortex stretches azimuthally and its local strength is decreasing, as indicated by the increase of the PV at the vortex center in going from Panels (a) to (c) of Fig. 5. The azimuthally averaged radial profile of PV between  $T = 5000$  and  $T = 13500$  does not show much difference for  $(r - r_p)/h > 12$ . In fact, the PV minimum at  $T = 10000$  is even slightly deeper than the one at  $T = 5000$ . At late time ( $T \geq 10^4$ ), while both the disk surface density and average PV profiles have changed very small amount, the vortex is getting narrower radially and is gradually being damped.

#### 4. DISCUSSION AND SUMMARY

We have considered the interaction of gaseous protoplanetary disks with high mass planets that are in circular orbits with orbital frequency  $\Omega_p$  and radius  $r_p$  from a central star. We have sampled the parameter space of different planet masses, different disk viscosities, and different disk temperatures and investigated how these parameters affect the lifetimes of disk vortices. We find that higher planet mass generally leads to longer vortex lifetimes, given the same disk viscosity and temperature. This result occurs because a more massive planet carves

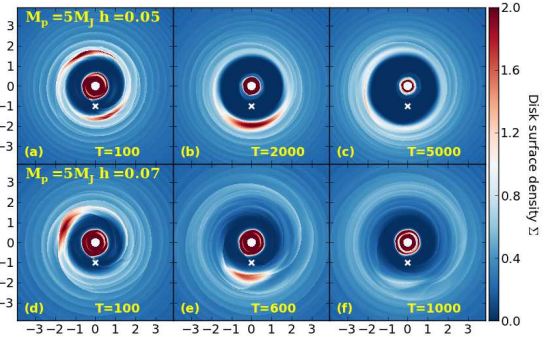


FIG. 2.— Similar to Fig. 1 except we now fix  $M_p = 5M_J$  and vary disk temperatures ( $c_s/(r\Omega) = h = 0.05, 0.07$ ). Again, both runs employ disk viscosity  $\nu = 1 \times 10^{-7} r_p^2 \Omega_p$ . Together with Fig. 1(d-f), we see the vortex lifetime is not monotonic with the disk temperature. (Color online)

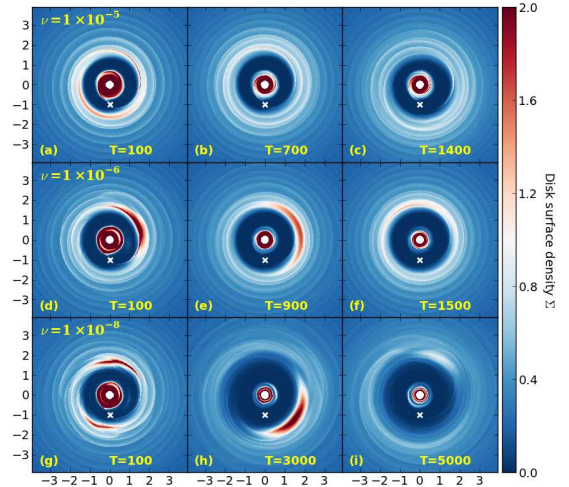


FIG. 3.— Similar to Fig. 1, except that we fix the planet mass as  $5M_J$  and disk temperature  $c_s/(r\Omega) = h = 0.06$  but vary disk viscosities ( $\nu = 10^{-5}, 10^{-6}, 10^{-8} r_p^2 \Omega_p$ ). Together with Fig. 1(d-f), we see the vortex lifetime is not monotonic with disk viscosity. (Color online)

out a cleaner gap and promotes a stronger RWI at the gap edge. Both disk viscosity and disk temperature have nonmonotonic effects on the vortex lifetime. We find that the optimal viscosity and dimensionless disk temperature values for vortex longevity are  $\nu = 10^{-7} r_p^2 \Omega_p$  ( $\alpha \simeq 3 \times 10^{-5}$ ) and  $h = 0.06 r_p$ . Higher or lower values of  $\nu$  or  $h$  would either shorten the vortex lifetime or inhibit vortex formation (see Fig. 4). In all our runs, we do not see the “return” of the vortex after its disappearance.

We do not believe that the lifetimes of the vortices in our simulations are determined by viscous damping because all our runs have vortex lifetimes that are significantly shorter than the viscous timescale on the vortex scale. In addition, we find that even lower viscosity (e.g.,  $\nu \sim 10^{-8}$ ) actually results in shortened vortex lifetimes. Instead, we speculate that the vortex is damped by shocks. Several competing effects are at play which jointly determine the evolution and lifetime of the vortex. For lower viscosity or lower temperature, on one hand, a higher mass planet is able to create a sharper gap edge and thus form stronger disk vortices. However, they also enhance spiral shocks that act to damp the vortex. For high viscosity or high temperature, shocks produced by

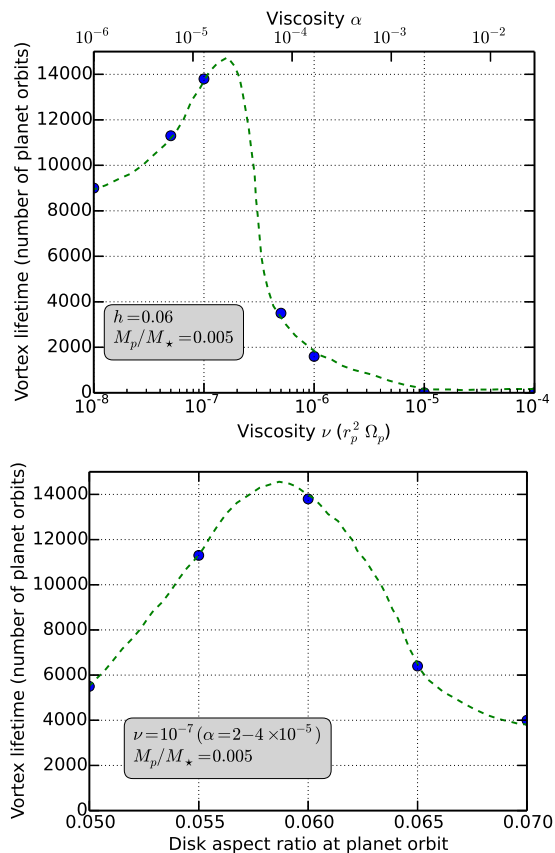


FIG. 4.— Disk vortex lifetime (in units of number of planet orbits) as a function of viscosity at fixed  $h = 0.06r_p$  (top) and temperature at fixed  $\nu = 1 \times 10^{-7}$  (bottom). A vortex is deemed “dead” after either the averaged azimuthal density variation or the averaged azimuthal potential vorticity variation within 10H (scale height) wide band around the vortex drops below 10%. The dashed lines are rough interpolations.

the planet are weaker but the planet cannot create a sharp edge. Consequently, in this regime the planet either does not induce vortex formation at all or it only excites a weak vortex which damps quickly. Therefore, intermediate values for disk viscosity and temperature provide the longest lived vortices that nearly balance the driving with damping of disk vortex.

Our findings can be compared with several recent observations. The longest vortex lifetime we find is  $\sim 10^4$  orbits for  $M_p = 5M_J$ ,  $\nu = 1 \times 10^{-7} r_p^2 \Omega_p$ , and  $h = 0.06r_p$ . The vortex is located at  $r = 2r_p$ . For the other sets of parameters that we have tried, the vortex lifetime spans from 0 to a few  $\times 10^3$  orbits. To explain relatively large disk gaps with dust emission asymmetries (Casassus et al. 2013; Fukagawa et al. 2013), the planet needs to be located far from the central star. For a slightly smaller hole as seen in Oph IRS 48, if we take the planet to be located at a radius of 20 AU, then the vortex is located at about 40 AU, and the disk inner gap has radius  $\sim 35$  AU. Then the longest vortex lifetime we simulated implies that this vortex can live for up to  $10^6$  yrs (assuming that the central star is one solar mass). Interestingly, these conditions are very similar to those found in the recent ALMA images of the disks around star Oph IRS 48 (van der Marel et al. 2013) and stars SAO 206464, SR 21 (Pérez et al. 2014).

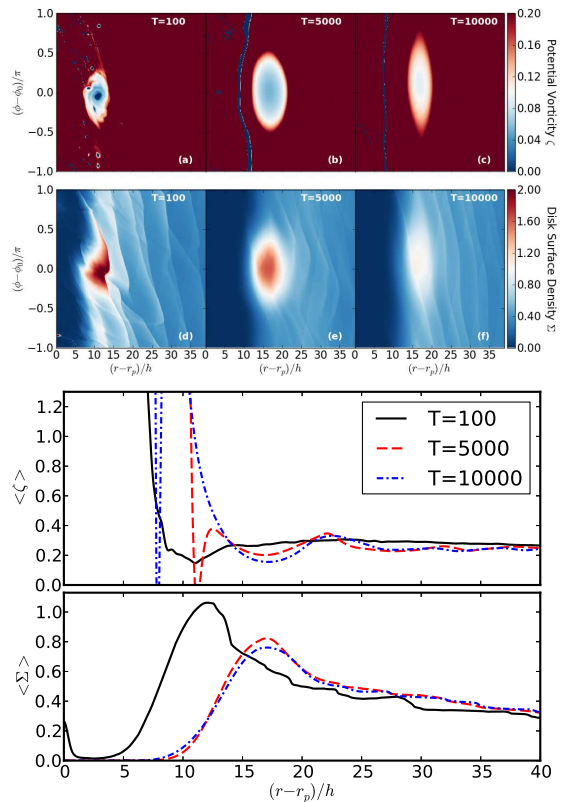


FIG. 5.— (Top) Color contours of disk potential vorticity and surface density distributions at different times for the run with planet mass  $M_p = 5M_J$ , viscosity  $\nu = 10^{-7} r_p^2 \Omega_p$ , and dimensionless disk temperature  $c_s/(r\Omega) = h = 0.06$ . Time is in units of the planet orbital period.  $\phi_0$  is the azimuthal coordinate of vortex center. (Bottom) Azimuthally averaged disk potential vorticity and surface density profiles for the same times as the upper plots. (Color online)

The Rossby wave/vortex instability is due to the gas. But its interaction with the dust leaves observable signatures as seen by ALMA. To better connect with observations such as ALMA images, one needs to also model the dust dynamics and radiative transfer. It has been suggested that dust can remain concentrated after the gas vortex has decayed (Birnstiel et al. 2013). We assume that gas and dust vortex lifetimes are roughly equal. Our preliminary results (not described here) suggest they are within 30% of each other. The disk vortex needs to last for  $\sim 10^6$  yrs in order to be responsible for the dust emission asymmetry in ALMA images of transition disks. As we have shown before, the dust asymmetry at  $\sim 40$  AU can survive for  $10^6$  yrs, but in a very small range of our simulation parameters. For dust asymmetry at  $\sim 100$  AU, the required number of orbits reduces to a few  $\times 10^3$  orbits that can be realized for a broader range of disk parameters. Due to the resolution of current ALMA configuration, all of the dust asymmetries are found to be far from the central star. With the most extended ALMA configuration, future observations will be able to resolve disk feature on scales closer to the central star. On-going exoplanet surveys (Brandt et al. 2014) could also shed light on the direct detection of forming massive planets in disks with these asymmetry features.

At a large orbital radius ( $\sim 50$  AU), the very low disk viscosity value ( $\nu = 10^{-7} r_p^2 \Omega_p$  or  $\alpha = 10^{-4}$  at  $r = 2$

where the vortex is located) for vortex longevity implies that this region does not evolve viscously over the disk lifetime. Such a low viscosity requires some explanation. In the T Tauri phase, the observationally inferred accretion rates onto the central star suggest that  $\alpha \sim 10^{-2}$  (Hartmann 1998). At that level of turbulence, we do not expect that vortices can form. The magneto-rotational instability (MRI) is a likely source of turbulence in the outer regions of a protoplanetary disk (Balbus & Hawley 1991). MRI typically results in an  $\alpha$  value  $\alpha \gtrsim 0.01$  that is again too high to permit the development of a vortex. On the other hand, the efficiency of MRI is weakened considerably in certain regions of protostellar disks due to nonideal MHD effects that result from the low levels of ionization (e.g. Bai & Stone 2011). Recent simulations by Zhu & Stone (2014) indicate that sufficiently low levels of  $\alpha$  and long vortex lifetimes can be achieved through the nonideal effects of ambipolar diffusion. The reconciliation of the low vis-

cosity requirements of vortex generation with the high viscosity requirement of accretion is unclear, possibly involving alternate accretion mechanisms.

The results presented here represent some preliminary steps in trying to understand the joint evolution of planet, disk accretion, vortices and dust asymmetries in the outer parts of the protoplanetary disk. Dust-gas interaction, disk self-gravity, more sophisticated viscosity profile, 3D structure could all affect disk vortex evolution to some extent. We plan to address these issues in future studies.

## ACKNOWLEDGEMENTS

Simulations in this work were performed using the Institutional Computing Facilities at LANL. WF, HL and SL gratefully acknowledge the support by the LDRD and IGPP programs and DOE/Office of Fusion Energy Science through CMSO at LANL. WF and SL acknowledge support from NASA grant NNX11AK61G. We thank Til Birnstiel and Zhaohuan Zhu for valuable comments.

## REFERENCES

- Andrews, S. M., Wilner, D. J., Espaillat, C., et al. 2011, *ApJ*, 732, 42
- Ataiee, S., Pinilla, P., Zsom, A., et al. 2013, *A&A*, 553, L3
- Bai, X. & Stone, J. M. 2011, *ApJ*, 736, 144
- Balbus, S. A. & Hawley, J. F. 1991, *ApJ*, 376, 214
- Barge, P. & Sommeria, J. 1995, *A&A*, 295, L1
- Birnstiel, T., Dullemond, C. P. & Pinilla, P. 2013, *A&A*, 550, L8
- Brandt, T. D., McElwain, M. W., Turner, E. L., et al. 2014, *ApJ*, submitted
- Casassus, S., van der Plas, G., Perez M., S., et al. 2013, *Nature*, 493, 191
- de Val-Borro, M., Artymowicz, P., D'Angelo, G. & Peplinski, A. 2007, *A&A*, 471, 1043
- Dobinson, J., Leinhardt, Z. M., Dodson-Robinson, S. E. & Teanby, N. A. 2013, *ApJ*, 777, L31
- Dodson-Robinson, S. E. & Salyk, C. 2011, *ApJ*, 738, 131
- Espaillat, C., D'Alessio, P., Hernández, J., et al. 2010, *ApJ*, 717, 441
- Forrest, W., Sargent, B., Furlan, E., et al. 2004, *ApJS*, 154, 443
- Fukagawa, M., Tsukagoshi, T., Momose, M., et al. 2013, *PASJ*, 65, L14
- Hartmann, L. 1998, *Accretion processes in star formation* (Cambridge: Cambridge University Press)
- Inaba, S. & Barge, P. 2006, *ApJ*, 649, 415
- Isella, A., Pérez, L. M., Carpenter, J. M., et al. 2013, *ApJ*, 775, 30
- Johansen, A., Anderson, A. C. & Brandenburg, A. 2004, *A&A*, 417, 361
- Kraus, A. L. & Ireland, M. J. 2012, *ApJ*, 745, 5
- Kraus, S., Ireland, M. J., Sitko, M. L., et al. 2013, *ApJ*, 768, 80
- Li, H., Colgate, S. A., Wendroff, B. & Liska, R. 2001, *ApJ*, 551, 874
- Li, H., Finn, J. M., Lovelace, R. V. E. & Colgate, S. A. 2000, *ApJ*, 533, 1023
- Li, H., Lubow, S. H., Li, S. & Lin, D. N. C. 2009b, *ApJ*, 690, L52
- Li, H., et al. 2005, *ApJ*, 624, 1003
- Lin, D. N. C. & Papaloizou, J. 1986a, *ApJ*, 307, 395
- Lin, D. N. C. & Papaloizou, J. 1986b, *ApJ*, 309, 846
- Lin, M-K. 2012, *MNRAS*, 426, 3211
- Lin, M-K. 2014, *MNRAS*, 437, 575
- Lin, M-K. & Papaloizou, J. 2011, *MNRAS*, 415, 1426
- Lovelace, R. V. E., Li, H., Colgate, S. A. & Nelson, A. F. 1999, *ApJ*, 513, 805
- Lyra, W. & Lin, M-K. 2013, *ApJ*, 775, 17
- Lyra, W. & Mac Low, M-M. 2012, *ApJ*, 756, 62
- Meheut, H., Casse, F., Varniere, P. & Tagger, M. 2010, *A&A*, 516, A31
- Meheut, H., Keppens, R., Casse, F. & Benz, W. 2012a, *A&A*, 542, A9
- Meheut, H., Meliani, Z., Varniere, P. & Benz, W. 2012b, *A&A*, 545, A134
- Meheut, H., Yu, C. & Lai, D. 2012c, *MNRAS*, 422, 2399
- Meheut, H., Lovelace, R. V. E. & Lai, D. 2013, *MNRAS*, 430, 1988
- Pérez, L. M., Isella, A., Carpenter, J. M. & Chandler, C. J. 2014, *ApJ*, 783, L13
- Pinilla, P., Birnstiel, T., Ricci, L., et al. 2012, *A&A*, 538, A114
- Regály, Z., Sándor, Z., Csomós, P. & Ataiee, S. 2013, *MNRAS*, 433, 2626
- Rice, W. K. M., Armitage, P. J., Wood, K. & Lodato, G. 2006, *MNRAS*, 373, 1619
- Richard, S., Barge, P. & Le Dizès, S. 2013, *A&A*, 559, 30
- Rosenfeld, K. A., Andrews, S. M., Wilner, D. J., Kastner, J. H. & McClure, M. K. 2013, *ApJ*, 775, 136
- Ruge, J. P., Wolf, S., Uribe, A. & Klahr, H. H. 2013, *A&A*, 549, 97
- van der Marel, N., van Dishoeck, E. F., Bruderer, S., et al. 2013, *Science*, 340, 1199
- Yu, C., Li, H., Li, S., Lubow, S. H. & Lin, D. N. C. 2010, *ApJ*, 712, 198
- Zhu, Z., Nelson, R. P., Hartmann, L., Espaillat, C. & Calvet, N. 2011, *ApJ*, 729, 47
- Zhu, Z., Nelson, R. P., Dong, R., Espaillat, C. & Hartmann, L. 2012, *ApJ*, 755, 6
- Zhu, Z., Stone, J. M., Rafikov, R. R., Bai, X. 2014, *ApJ*, 785, 122
- Zhu, Z. & Stone, J. M. 2014, *ApJ*, submitted